Review Article

Strengths and limitations of tractography methods to identify the optic radiation for epilepsy surgery

Ylva Lilja[1], Daniel T. Nilsson[1,2]

[1]Department of Clinical Neuroscience and Rehabilitation, Institute of Neuroscience and Physiology, The Sahlgrenska Academy, University of Gothenburg, Gothenburg, Sweden; [2]Department of Neurosurgery, Sahlgrenska University Hospital, Gothenburg, Sweden

Correspondence to: Ylva Lilja, MD. Ear, Nose and Throat Clinic, Sahlgrenska University Hospital, Gröna Stråket 5, 413 45 Göteborg, Sweden. Email: ylva.lilja@neuro.gu.se.

Abstract: Diffusion tensor imaging (DTI) tractography (TG) can visualize Meyer's loop (ML), providing important information for the epilepsy surgery team, both for preoperative counseling and to reduce the frequency of visual field defects after temporal lobe resection (TLR). This review highlights significant steps in the TG process, specifically the processing of raw data including choice of TG algorithm and the interpretation and validation of results. A lack of standardization of TG of the optic radiation makes study comparisons challenging. We discuss results showing differences between studies and uncertainties large enough to be of clinical relevance and present implications of this technique for temporal lobe epilepsy surgery. Recent studies in temporal lobe epilepsy patients, employing TG intraoperatively, show promising results in reduction of visual field defects, with maintained seizure reduction.

Keywords: Temporal lobe resection (TLR); epilepsy surgery; Meyer's loop (ML); optic radiation; visual field defect; tractography (TG); diffusion tensor imaging (DTI)

Submitted Nov 24, 2014. Accepted for publication Jan 22, 2015.
doi: 10.3978/j.issn.2223-4292.2015.01.08
View this article at: http://dx.doi.org/10.3978/j.issn.2223-4292.2015.01.08

Introduction

More than one third of patients with temporal lobe epilepsy are resistant to drug therapy (1). Temporal lobe resection (TLR) is a well-established treatment for this group resulting in a high frequency of sustainable seizure freedom with low morbidity (2,3). Fifty to 90% of patients who undergo TLR suffer a post-operative visual field defect, due to injury to the most anterior part of the optic radiation, Meyer's loop (ML) (4,5). A large enough visual field defect due to TLR can lead to ineligibility to drive, which is reported to afflict 4% to 50% of patients despite of being seizure free (6-9). Evaluations have shown that the ability to drive is one of the most important goals for patients considering epilepsy surgery (6,10).

ML is located in the anterior part of the temporal lobe, adjacent to other white matter pathways, including the uncinate fasciculus, the inferior longitudinal fasciculus and the inferior occipito-temporal fasciculus. It cannot be visually separated from other white matter structures by the human (surgeon's) eye, nor by conventional imaging techniques. However, with recent advances in fiber tractography (TG) by diffusion tensor imaging (DTI), ML can be visualized *in vivo*. Possible applications for TG include delineating the optic radiation before TLR, in order to assess the risk of developing a visual field defect as well as for intraoperative use, to avoid injury to ML and thus postoperative visual field defects.

This review summarizes the current status of TG and its possibilities for TLR from a clinical perspective. Although a promising technique, there are important limitations that, if not appreciated, may result in neurological injury. We discuss results showing differences between studies and uncertainties large enough to be of clinical relevance and present implications of this technique for temporal lobe epilepsy surgery.

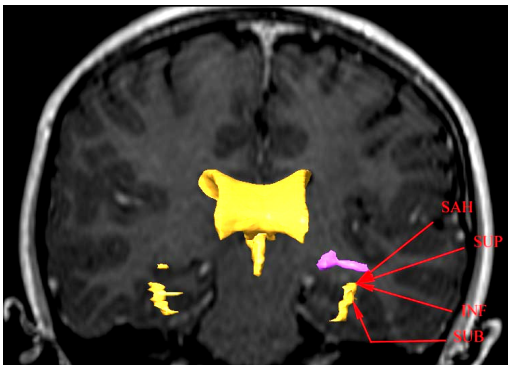

Figure 1 Surgical approaches-relationship between Meyer's loop and the temporal horn. Coronal T1-weighted MRI showing the relationship between Meyer's loop (in pink) and the temporal horn of the lateral ventricle (in yellow). The angles of approach to the temporal horn for: a SAH, TLR through the SUP, TLR through an INF, and the SUB. SAH, selective amygdalohippocampectomy; TLR, temporal lobe resection; SUP, superior temporal gyrus; INF, inferior approach; SUB, subtemporal approach.

Implications for temporal lobe epilepsy surgery

The aim of surgery for medically refractory mesial temporal lobe epilepsy is to resect the epileptogenic zone, i.e., the hippocampus, parahippocampal gyrus and amygdala. Three types of resections predominate in reports from epilepsy surgery centres: classical anterior TLR, modified anterior TLR and amygdalohippocampectomy (transsylvian or transcortical) (11,12).

All three techniques require the identification and opening of the temporal horn of the lateral ventricle to identify and remove the medial temporal lobe structures (*Figure 1*). Hence visual field defects are common not only after TLR, but also after amygdalohippocampectomy, occurring in 79% in transcortical amygdalohippocampectomy as compared to 73% in lateral TLR in the same study (5). Selective amygdalohippocampectomy (SAH) has similar results with 83% of the patients developing a partial or complete quadrantanopia (13).

How can we reduce the risk of a postoperative visual field defect following temporal lobe epilepsy surgery? Both the anatomical configuration of ML, as an outward slanting roof of the lateral ventricle, and the interindividual variation in the position of ML need to be considered. By selecting a more inferior approach (INF) to the temporal horn of the lateral ventricle, the risk of injury to the optic radiation can be decreased. The most extreme application of this is the subtemporal approach (SUB) through the inferior temporal sulcus to the hippocampus. No visual field defect after TLR, using this approach in seven patients, has been reported (14). A study comparing transsylvian, transtemporal and SUB to tumours in the mesial temporal lobe found no visual field defects with the SUB, but, new or worsened deficits in 20-45% of patients with the other two approaches (15). However, the SUB has other disadvantages such as the risk for temporal contusions, small field of view, and sometimes the need for resection of the zygomatic arch. By using an anterior-INF to open the temporal horn in TLR, rather than the superior-lateral one, which passes through the optic radiation, a visual field defect may be avoided. Visualization of the optic radiation using TG implemented in a neuronavigation system could guide the surgeon to the angle of approach to the temporal horn and thus the extent of resection to avoid injury to ML.

Meyer's loop (ML)

The visual pathways start at the retina of the eyes and extend posteriorly, first as the anterior visual pathway, which ends in the lateral geniculate nuclei of the thalamus. From here, the visual pathway continues as the optic radiation (also known as the geniculocalcarine tract), which extends posteriorly in three nerve bundles and ends in the primary visual cortex (VC) in the respective occipital lobe.

The anterior bundle that forms ML, was first identified as part of the optic radiation in 1906 by Archambault and later described more in detail by Meyer in 1907 (16,17). It extends anteriorly in the temporal lobe, spreading out in a thin sheet of fibers and turning sharply in a bend around the roof of the temporal horn of the lateral ventricle, before continuing posteriorly towards the occipital lobe. The anterior bundle, including ML, represents the superior quadrant of the contralateral visual field, and thus a complete injury to the structure during surgery results in a contralateral quadrantanopia (16,18).

In more recent studies, the architecture of the optic radiation has primarily been explored and determined by dissection studies, using Klingler's fiber dissection technique (19) (*Figure 2*). In the Klingler dissection process, a formalin-fixed human cadaver brain is frozen and returned back to room temperature several times. Growing ice crystals separate the nerve fibers slightly, allowing them to be dissected from each other. Anatomical data from these studies are often considered the gold standard of white matter anatomy and are thus often used to evaluate

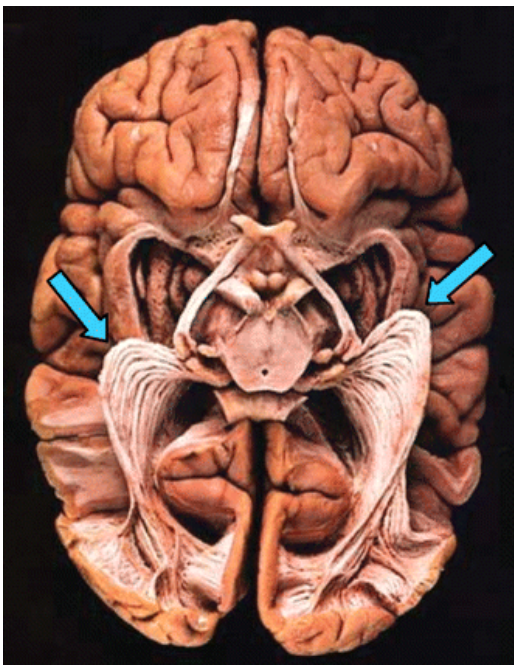

Figure 2 The optic radiation exposed (virtual hospital). A brain seen from below, prepared using Klingler's fiber dissection technique. Meyer's loop is indicated by the arrows.

anatomical accuracy of other techniques, including DTI TG.

Ebeling and Reulen [1988] dissected 25 brains and concluded a distance between the temporal pole and the anterior limit of ML (TP-ML) of 27±3.5 mm (range, 22-37 mm) (20). Other dissection studies have found similar results and have also confirmed the considerable interindividual variation of the anterior extent of ML (20-23). Furthermore, studies have shown an interhemispheric asymmetry of the anterior extent of ML with a more anterior location in the left temporal lobe (9,24). It has been proposed that this is due to expanding language areas in the left posterior temporal lobe, displacing ML forwards on this side. Based on this variability in location of ML, a general safety limit of resection size for TLR cannot be specified. Instead, individualized risk calculations have to be made in order to prevent visual field defects.

Diffusion tensor imaging (DTI) and tractography (TG)

Conventional diffusion MRI normally applies three gradient directions to model the diffusion in each voxel as a sphere and detect the amount of water diffusion. DTI is a variety of diffusion MRI that, by applying six or more gradient directions, models the diffusion in each voxel as an ellipsoid, and thus can detect both the amount and the directionality of diffusion. From this information the main direction of water diffusion and the size of the main water diffusion vector per voxel can be determined (25). The main direction of water diffusion has been shown to reflect the direction of the regional white matter tracts (26). Degree of directionality can be calculated and is frequently expressed as fractional anisotropy (FA), where FA =0 signifies complete isotropy (as in CSF) and FA values closer to 1 signifies high anisotropy (typically around 0.7 in well organized, healthy white matter tracts).

By connecting voxels based on their anisotropy and their principal diffusion direction, images of the major white matter pathways can be constructed. This is referred to as fiber tracking or TG (25,27-29). DTI TG has important clinical applications in neurosurgery including preoperative planning and intraoperative delineation of major white matter tracts (26,30-37).

The tractography (TG) process and Meyer's loop (ML)

The TG process includes several steps, and in each step there are several variable factors to determine (*Figure 3*). First data is collected using a DTI protocol in the MRI scanner. The raw data from the MRI scanner is then processed and adjusted by one of several available software programs. Finally, the TG algorithm with different threshold settings is chosen, and regions of interest (ROIs) are defined as start, and waypoints for the TG. To this date, there is no consensus about how TG should be performed, including all the variables mentioned above, and TG studies thus differ in many ways, which affect the results and should be taken into consideration when comparing results. It is realistic to assume that the "best" way to produce TG, in order to achieve anatomically correct visualizations, varies depending on which tract is to be delineated, as different tracts have different qualities, regarding thickness, shape and surrounding tissue.

Data collection

Several variable factors in the raw data collection in the MRI scanner can affect the final TG result significantly. Limitations and pitfalls in the scanning procedure have

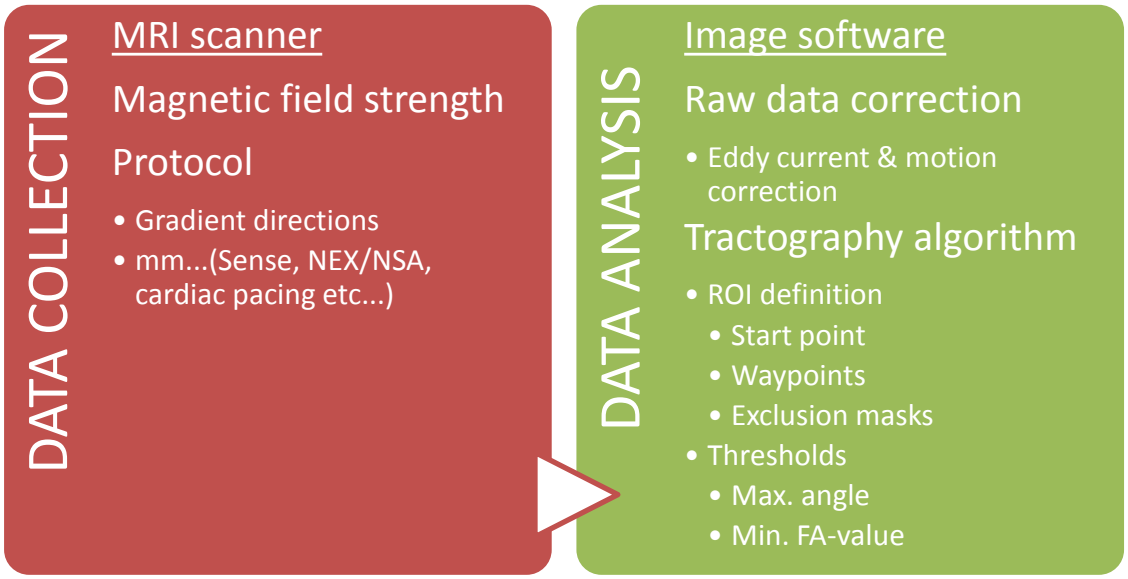

Figure 3 Flow chart of the tractography process. The tractography process includes several steps, each one with several variable factors. The first part (red square) is the raw data collection, including choice of MRI scanner and protocol settings. The aim is to maximize information while minimizing noise and artifacts. The second part (green square) is the raw data analysis, including data correction steps, choice of tractography algorithm with specific threshold settings and definition of start, way and exclusion masks (ROIs) to guide the tracking. NEX, number of excitations; NSA, number of signal averages; ROI, region of interest; FA, fractional anisotropy.

been discussed in detail previously and will not be covered herein (38). However, we choose to briefly mention two matters of controversy and significance for the end result.

Although most would agree that the doubled signal strength at 3 T as compared to 1.5 T is desirable, it is a complicated matter of scanner specifications, which must be considered. An important issue to specifically consider in the case of DTI and the anterior part of the temporal lobe is scan artifacts due to susceptibility. Susceptibility artifacts are the result of microscopic gradients or variations in the magnetic field strength that occur near the interfaces of tissue/substance of different magnetic susceptibility (e.g., soft tissue, bone, air filled cavities), such as close to the sinuses. The result is geometric image distortion and signal loss in such regions (39,40). When the magnetic field strength increases from 1.5 to 3 T the effects of susceptibility doubles and thus the net result at 3 T is more troublesome artifacts in the images than at 1.5 T. Possible remedies are increased parallel imaging acceleration, reduced field of view and segmented k-space scanning, each of which comes at a cost in terms of signal, scan time and technical complexity.

The optimal number of gradient directions for TG has been discussed and there seems to be a general perception that more directions is better. However, there is little support for this perception in the literature, apart from an expected increase in signal-to-noise ratio purely due to the fact that more directions necessitate more measurements to be performed. Both simulation and *in vivo* studies indicate that in practice there is little to be gained in using more than 16 directions (41,42). Yamamoto *et al.* [2007] compared different numbers of gradient directions-using 6, 12, 40 and 81 directions—and found no difference in visualization of the optic radiation (43).

The tractography (TG) algorithm

The raw data from the MRI scanner is transferred to a computer for processing.

There are several different image softwares available; some are freeware and some are included in MRI scanner or neuronavigation packages. First, for all DTI data, correction for eddy current and motion effects during the scan should be carried out. Next, DTI images are calculated, including FA-map, eigen-value and vector images. Based on the information of these images, TG can be performed through different algorithms. The two most common TG algorithms for clinical ML studies and use to this date are

deterministic (DTG) and probabilistic TG (PTG).

Deterministic, or streamline, TG techniques assume that the orientation within a voxel is precisely known. A tract is produced by defining a start point and applying an algorithm linking voxels with similar diffusion directions (29). The technique can be refined by applying threshold criteria, such as minimum FA-value of a tract voxel and maximum angle of deviation of diffusion direction between voxels. Multiple ROIs are defined, to specify where the tract must pass, a technique known as "virtual fiber dissection" (44). The advantages of DTG are relatively simple calculations and fast results with a clear delineation of fiber tracts, and the main limitations are operator-dependency, difficulties resolving curving, crossing or kissing tracts and that there is no indication of the confidence that one can assign to a reconstructed trajectory (29).

In contrast to deterministic techniques, PTG calculates the uncertainty of diffusion orientation within each voxel. It then traces a large number of (typically >5,000) possible pathways from a set starting point (29). The result is a probability distribution of connections and by selecting an appropriate threshold, below which connections are discarded as unlikely, tracts can be outlined. PTG is less likely to exclude voxels with low FA due to, for example, crossing fibers or scan artifacts. However, PTG requires long calculation times and, furthermore, the algorithm is not as widely supported by the MRI scanner manufacturers' own software as is DTG. Thus, third party software is required for PTG, which adds complexity to the TG process.

New methods may improve clinical TG in the near future. Modeling the diffusion distribution in each voxel as a 3×3 symmetric tensor is the most common approach in the DTI community today, and indeed in existing clinical studies, which is the focus of the discussions of this review. However, this modeling is not able to resolve complex intra-voxel micro-structures (e.g., crossing fibers), which are deemed to exist in at least one third of all white matter (45). In order to address this problem a wide variety of multi-fiber diffusion models have been proposed including 'ball and stick' model (46), analytical q-ball imaging (47) and non-negativity constrained spherical deconvolution (CSD) (48). A recent review has evaluated and compared six different analysis methods in terms of false-positive and false-negative fiber detection rates and reports that CSD has the best fiber detection rates (49). CSD has also been shown to successfully visualize the optic radiation including ML (50).

The tractography (TG) algorithm, thresholding and Meyer's loop (ML)

ML is a challenging structure for TG due to anatomical factors mentioned above: first, its location in close vicinity to other white matter tracts and, second, its thin and sharply bending shape. Voxels in the DTI scan are typically 1-2 mm in each dimension and thus contain a large amount of neurons each; the diameter of a single neuron is approximately 0.01 mm. This means that a single voxel can contain axons with different directions (i.e., different main diffusion directions) if it is located across parts of different pathways that are crossing, "kissing" (= pass adjacent to each other) or if a single pathway is curving within the voxel.

Nevertheless, several TG studies have successfully visualized ML (see *Table 1*) (24,51-59). All these studies confirm the inter-individual difference of the anterior extent of ML (TP-ML) in the temporal lobe, also found in dissection studies. However, the mean and range of TP-ML differ between studies, as well as several variables in the TG process. The question remains as to how to validate the anatomical accuracy of TG in the living human brain, to find out which, or if, any of these TG methods are reliable enough to be used in the clinical reality.

In the discussion about study results below, focus is on the TP-ML distance (*Figure 4*). Although other shape and location qualities than the anterior extent of ML may be relevant, TP-ML is considered the most important measure intraoperatively, since this is the part most prone to injury during TLR. Also, the qualities of the anterior-most part of ML makes it the most technically challenging part and could thus be an indicator of success of the TG method.

Several TG studies of ML have validated their results by comparison to the gold standard, dissection studies by Klingler's technique. Judging from these comparisons, all TG studies to this date seem to underestimate the anterior extent of ML (20-23) (*Table 1*). However, in the majority of the TG studies, PTG places ML more anteriorly than DTG, with resulting TP-ML measures closer to results of dissection studies. The reason could be differences in the algorithms, where PTG may be better able to cope with crossing and kissing fibers than deterministic models because it allows uncertainty of diffusion orientation and thus is less likely to exclude voxels with low FA, and interrupt tracking at such voxels (29,56). As ML has a curving shape and the optic radiation is adjacent to several other white matter tracts, DTG may thus be suboptimal for TG of the optic radiation.

Table 1 The anterior extent of Meyer's loop-results as reported from cadaver dissection and tractography studies

Author/year	Study population	Measurement technique	TP-ML (mm): mean [range]
Peuskens *et al*., 2004 (22)	17 controls	Cadaver dissection	27 [15-30]
Ebeling and Reulen, 1988 (20)	25 controls	Cadaver dissection	27 [22-37]
Chowdhury and Khan, 2010 (21)	11 hemispheres	Cadaver dissection	26 [23-31]
Rubino *et al*., 2005 (23)	20 controls	Cadaver dissection	25 [22-30]
Yamamoto *et al*., 2005 (51)	5 controls	DTG	37 [33-40]
Nilsson *et al*., 2007 (52)	7 controls, 2 patients	DTG	Controls: 44 [34-51]; patients: 46 [40-51]
Taoka *et al*., 2008 (53)	14 patients	DTG	37 [30-43]
Chen *et al*., 2009 (54)	48 patients	DTG	32 [21-51]
Dreessen de Gervai *et al*., 2014 (24)	20 controls	DTG	43 [28-54]
Sherbondy *et al*., 2008 (55)	8 controls	PTG	28 [25-31]
Yogarajah *et al*., 2009 (56)	21 controls, 20 patients	PTG	Controls: 35 [24-47]; patients: 34 [24-43]
Anastasopoulos *et al*., 2014 (57)	10 patients	DTG, PTG	DTG, depicted in 3/10 patients: 41 [39-43]; PTG, depicted in 9/10 patients: 34 [23-40]
Lilja *et al*., 2014 (58)	11 controls	DTG, PTG	DTG: 44 [34-51]; PTG: 33 [25-48]
Borius *et al*., 2014 (59)	13 controls, 18 patients	DTG, PTG	DTG: 26; PTG: 30

TP-ML, distance between temporal pole and anterior delineation of Meyer's loop; TG, tractography; DTG, deterministic TG; PTG, probabilistic TG.

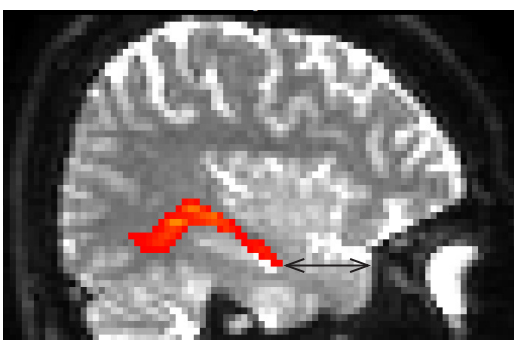

Figure 4 Measuring TP-ML. TP-ML, the distance between the temporal pole and the anterior delineation of Meyer's loop, measured as demonstrated with arrow.

However, there are many variables in the TG process that can influence the resulting tract. Also, most DTI studies have small study populations (typically 10-20 subjects). Thus, differences found in comparisons between studies could have many explanations. Three studies have compared probabilistic and deterministic algorithms applied on the same set of DTI scans (57-59). Anastasopoulos *et al*. [2014] and Lilja *et al*. [2014] found very similar TP-ML results: measures by DTG placed ML close to 1 cm more posteriorly than measures by PTG, and the latter one approximately 1 cm more posteriorly than dissection studies. It should be pointed out that Anastasopoulos *et al*. based their deterministic results on very few subjects (n=3), because this algorithm failed to depict ML in most subjects in their study. Borius *et al*. [2014] found the opposite relation, with tractographies placing ML more anteriorly using DTG than PTG. However, the maximum angle allowed between the main diffusion directions of two voxels was unusually small for PTG—approximately 37 degrees—whereas most studies use an angle around 90 degrees. This factor most likely affects the tracking in the sharply bending region of ML extensively, why these TP-ML results should not be compared with other probabilistic studies.

The implication of the angle threshold highlights the importance of threshold settings and their effect on ML. The effect of FA threshold on the anterior extent of ML TG has also been discussed (used to determine below which FA value tracking should be stopped). Borius *et al*. compared three different FA thresholds—0.18, 0.20 and 0.22—and found no significant TP-ML differences. Chen *et al*. explored the location of ML using DTG with an FA threshold of 0.15; such a low FA threshold could increase the sensitivity of finding the most anterior fibers in a region where partial volume effects will occur (54). They

found TP-ML values as close to dissection studies as most studies employing PTG. Thus, it could be argued that the deterministic technique could produce similar results as the probabilistic one, if performed by experts in white matter anatomy, using adequate threshold settings.

Another factor to consider is the selection of ROIs, which define the start and end points, and in most cases also waypoints, for TG. In the majority of TG studies of ML, the ROIs are manually drawn based on the operators' prior anatomical knowledge; there is thus a factor of subjectivity in this step. Attempts to automate this step in patient cohorts have been made, but have not yet proven to be as successful as the manual method (60). This could be due to important individual anatomical differences and possible anatomical distortions in brains with pathology. Our group found a lower reproducibility between and within operators for DTG compared to PTG (58). In the deterministic process several additional, "trimming" ROIs have to be added to the standardized ones to exclude aberrant fibers, as opposed to the probabilistic process. These additional ROIs are selected by the operator, differently in each individual scan, resulting in several operator- and scan-specific ROIs. Subjectivity thus becomes a major issue in DTG of ML, and could explain the lower reliability.

Validation of tractography (TG) of Meyer's loop (ML)

Comparisons to gold standard

Following the discussion above, although some results are contradictory, results by PTG appear superior to DTG in anatomical validity and reliability. However, also the probabilistic results seem to underestimate TP-ML, in general placing ML almost 1 cm more posteriorly than dissection studies. However, it is possible that the error margin is not as large as 1 cm, as also the gold standard, Klingler's fiber dissection technique, has been questioned. A certain deformation level has been shown to occur during dissection, possibly due to the extraction of the brain from the cranium, shrinking of the tissue during fixation by formalin and fissuring of the tissue due to freezing. The deformation level has furthermore been shown to vary between different brain structures and regions. The specific deformation of the Meyer's-loop region is unknown; however, a global brain volume shrinkage of 8.1% has been reported (61). TP-ML measures from dissection studies may thus be artificially shorter than those of a living brain, which should be taken into account when evaluating the systematic difference seen in comparison to TG.

Other methods to achieve gold standard for white matter anatomy of the brain have been suggested, such as MRI-detectable neuronal tracers. Dyrby *et al*. compared results from manganese-enhanced imaging to PTG, and concluded that the latter reliably detected specific pathways, including the optic radiation (62). To ensure that most of the sources known to degrade accuracy of *in vivo* DTI TG, they performed their experiments on post mortem porcine brains. These results are promising, however, the accuracy of TG in *in vivo* human brains still remains to be determined.

Validation by prediction of postoperative outcome

Anatomical validation of ML TG of the living human brain is a challenge. Group comparison to dissection studies, of relatively small study populations as discussed above, is not convincing.

A few groups have attempted validation by using TG results (often TP-ML measures) to predict visual field outcome in patients who have undergone TLR (52-54,56,63,64). The prediction models have all been successful, however, to different degrees. Taoka *et al*., using DTG in a study of 14 TLR patients, found that pre-operative TP-ML and resection length together could divide their cohort into two groups: those with no or small visual field defects and those with larger visual field defects (53). Chen *et al*. could show a correlation between change in TP-ML width and visual field defect, using DTG in a study of 48 TLR patients (54). In a PTG study based on 20 TLR patients, Winston *et al*. found similar correlations and were able to predict degree of post-operative visual field defect, comparing resection length and pre-operative TP-ML (63). *Figure 5* is a case example of a patient who underwent TLR.

The studies described above prove a certain anatomical accuracy in TG of ML. Notably, however, a variety of TG parameters, as well as both deterministic and probabilistic algorithms, have been employed in these studies. As there are known differences in the ability of different TG varieties to depict the anterior extent of ML, one could assume these studies validate the accuracy of TG with a certain margin of error.

Tractography (TG) during temporal lobe resection (TLR)

An accurate validation of TG of ML is necessary for its safe

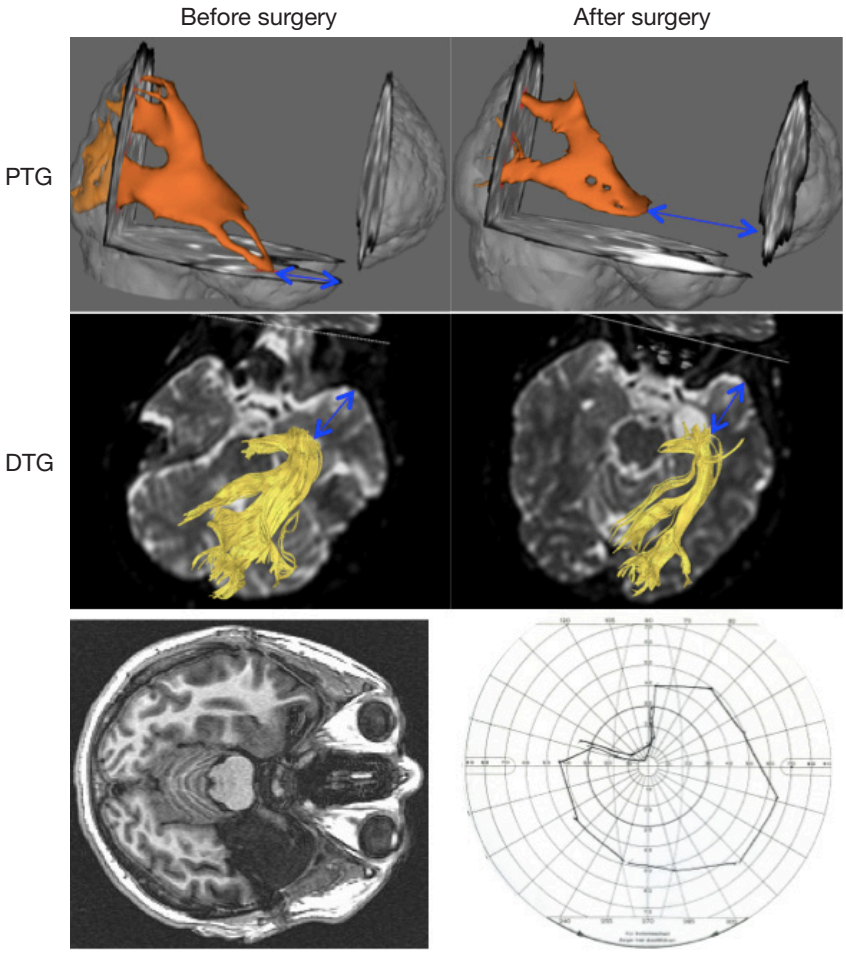

Figure 5 Case example-tractography in a TLR patient. This patient suffered a visual field defect after TLR. Tractography by PTG showed a significant increase of TP-ML after surgery, consistent with the visual defect, while no such change could be seen using DTG in this case. Upper row: PTG before (left) and after (right) TLR. Middle row: DTG before (left) and after (right) TLR. Blue arrows indicate the TP-ML. Lower row: post-operative T1 (left) and perimetry (right). TLR, temporal lobe resection; PTG, probabilistic tractography; TP-ML, distance between temporal pole and anterior delineation of Meyer's loop; DTG, deterministic tractography.

clinical use. All methods have their limitations: there is yet no convincing gold standard and all cadaver studies differ from the reality of the living human brain, in the tissue changes and physiological changes that occur post mortem. Also, the clinical reality includes practical factors like possible scanning time and individual differences, which are not replicated in lab settings. Thus, instead of testing the accuracy of TG, the end goal of decreasing/avoiding visual field defects for TLR cases by using TG could be tested directly.

Three studies to this date have reported results of pre- and intraoperative TG during TLR and the effect on postoperative visual outcome. Thudium *et al.* [2010] reported using preoperative TG in a surgical neuronavigation system in 12 patients, attempting to plan safe surgical trajectories of resection to avoid injury to ML (65). There was no control group in this study, however, 75% of the patients had no postoperative visual field defect, compared to 53% in a previous study from the same group.

Siu *et al.* [2012] reported results from the first prospective comparative study in this area (66). They compared visual outcome of TLR between a group of subjects where intraoperative TG guidance was used (n=15) and a control group where conventional intraoperative image guidance

was used (n=23). A total of 66% of the subjects in the TG group had no VFD versus 30% in the control group. However, limited information about methodology for both TG method and data analysis was published.

Winston *et al*. [2014] included 21 patients consecutively and displayed preoperative TG intraoperatively on a neuronavigation system and in the operation microscope (67). None of the 21 patients had a postoperative visual field defect that precluded driving, compared to 13% in a previous cohort of 44 patients. They concluded that intraoperative TG guidance for the surgeon reduces severity of visual outcome, while preserving level of seizure outcome. Further randomized prospective studies with control groups, and larger cohorts, are needed to confirm these findings.

The effect of brain shift during surgery, and thus the reliability of preoperative TG, has been questioned. Chen *et al*. [2009] measured brain shift intraoperatively and found a shift of up to 11 mm following craniotomy, with shift occurring in both the vertical and horizontal planes (54). Winston *et al*. [2014] explored the clinical significance of brain shift during surgery, and the possible need for adjustment of the preoperative TG. In the study described in the paragraph above, they carried out intraoperative MRI on twelve of the patients and coregistered the preoperative tractographies to these scans. They compared results to nine patients where the unchanged preoperative tractographies were used intraoperatively. No significant difference in visual field outcome was found between the two groups and thus they concluded that the time-consuming intraoperative scan might not be necessary.

Conclusions and future directions

DTI TG can visualize ML, providing important information to the epilepsy surgery team, both for preoperative counseling, and to reduce the frequency of visual field defects. This review highlights limitations and pitfalls of the TG process, from acquiring the DTI scan to the TG algorithm chosen and interpretation of the results. A lack of standardization of TG of the optic radiation makes study comparisons difficult. We highlight results showing differences between studies and uncertainties large enough to be of clinical relevance and present implications of this technique for temporal lobe epilepsy surgery. Recent studies in temporal lobe epilepsy patients, employing TG intraoperatively, show promising results in reduction of visual field defects, with maintained seizure reduction. Future development will include improvements in scanners, scan techniques and TG algorithms. Whether this will translate into a benefit for temporal lobe epilepsy patient remains to be seen. Further postmortem validation and clinical optimization of TG data as well as experimental confirmation of the benefits of TG of the optic radiation in temporal lobe epilepsy patients are needed.

Acknowledgements

We would like to thank MRI physicists Maria Ljungberg and Göran Starck for educational discussions and contribution to this review. We thank Professors Kristina Malmgren and Bertil Rydenhag for valuable cooperation and input.

Disclosure: The authors declare no conflict of interest.

References

1. Semah F, Ryvlin P. Can we predict refractory epilepsy at the time of diagnosis? Epileptic Disord 2005;7 Suppl 1:S10-3.
2. Wiebe S, Blume WT, Girvin JP, Eliasziw M, Effectiveness and Efficiency of Surgery for Temporal Lobe Epilepsy Study Group. A randomized, controlled trial of surgery for temporal-lobe epilepsy. N Engl J Med 2001;345:311-8.
3. Bjellvi J, Flink R, Rydenhag B, Malmgren K. Complications of epilepsy surgery in Sweden 1996-2010: a prospective, population-based study. J Neurosurg 2015;122:519-25.
4. Nilsson D, Malmgren K, Rydenhag B, Frisén L. Visual field defects after temporal lobectomy -- comparing methods and analysing resection size. Acta Neurol Scand 2004;110:301-7.
5. Egan RA, Shults WT, So N, Burchiel K, Kellogg JX, Salinsky M. Visual field deficits in conventional anterior temporal lobectomy versus amygdalohippocampectomy. Neurology 2000;55:1818-22.
6. Bjellvi J, Rydenhag B, Malmgren K. Visual field defects and permission to drive in adults after temporal lobe resections for epilepsy. Epilepsia 2014;55:4-246.
7. Manji H, Plant GT. Epilepsy surgery, visual fields, and driving: a study of the visual field criteria for driving in patients after temporal lobe epilepsy surgery with a comparison of Goldmann and Esterman perimetry. J Neurol Neurosurg Psychiatry 2000;68:80-2.
8. Pathak-Ray V, Ray A, Walters R, Hatfield R. Detection

of visual field defects in patients after anterior temporal lobectomy for mesial temporal sclerosis-establishing eligibility to drive. Eye (Lond) 2002;16:744-8.
9. Jeelani NU, Jindahra P, Tamber MS, Poon TL, Kabasele P, James-Galton M, Stevens J, Duncan J, McEvoy AW, Harkness W, Plant GT. 'Hemispherical asymmetry in the Meyer's Loop': a prospective study of visual-field deficits in 105 cases undergoing anterior temporal lobe resection for epilepsy. J Neurol Neurosurg Psychiatry 2010;81:985-91.
10. Taylor DC, McMacKin D, Staunton H, Delanty N, Phillips J. Patients' aims for epilepsy surgery: desires beyond seizure freedom. Epilepsia 2001;42:629-33.
11. Spencer DD, Spencer SS, Mattson RH, Williamson PD, Novelly RA. Access to the posterior medial temporal lobe structures in the surgical treatment of temporal lobe epilepsy. Neurosurgery 1984;15:667-71.
12. Yaşargil MG, Teddy PJ, Roth P. Selective amygdalo-hippocampectomy. Operative anatomy and surgical technique. Adv Tech Stand Neurosurg 1985;12:93-123.
13. Novak K KK, Pataraia K, Marschalek J, Reitner A, Baumgartner C, Czech T. Incidence of visual field defects following selective amygdalohippocampectomy. Epilepsia 2004;45:62.
14. Miyagi Y, Shima F, Ishido K, Araki T, Taniwaki Y, Okamoto I, Kamikaseda K. Inferior temporal sulcus approach for amygdalohippocampectomy guided by a laser beam of stereotactic navigator. Neurosurgery 2003;52:1117-23; discussion 1123-4.
15. Jiang ZL, Wang ZC, Jiang T. Surgical outcomes of different approaches for mesial temporal lobe gliomas. Zhonghua Yi Xue Za Zhi 2005;85:2428-32.
16. Meyer A. The connections of the occipital lobes and the present status of the cerebral visual affections. Trans Assoc Am Physicians 1907;22:7-16.
17. Archambault L. Le faisceau longitudinal inferieur et le faisceau optique central: Quelques considerations sur les fibres d´association du cerveau. Rev Neurol 1906;4:1206.
18. Harrington DO. Visual field character in temporal and occipital lobe lesions. Localizing values of congruity and incogruity in incomplete homonymous hemianopsia. Arch Ophthalmol 1961;66:778-92.
19. Klingler J. eds. Atlas Cerebri Humani. Basel: Karger, 1956.
20. Ebeling U, Reulen HJ. Neurosurgical topography of the optic radiation in the temporal lobe. Acta Neurochir (Wien) 1988;92:29-36.
21. Chowdhury FH, Khan AH. Anterior & lateral extension of optic radiation & safety of amygdalohippocampectomy through middle temporal gyrus: a cadaveric study of 11 cerebral hemispheres. Asian J Neurosurg 2010;5:78-82.
22. Peuskens D, van Loon J, Van Calenbergh F, van den Bergh R, Goffin J, Plets C. Anatomy of the anterior temporal lobe and the frontotemporal region demonstrated by fiber dissection. Neurosurgery 2004;55:1174-84.
23. Rubino PA, Rhoton AL Jr, Tong X, Oliveira Ed. Three-dimensional relationships of the optic radiation. Neurosurgery 2005;57:219-27; discussion 219-27.
24. Dreessen de Gervai P, Sboto-Frankenstein UN, Bolster RB, Thind S, Gruwel ML, Smith SD, Tomanek B. Tractography of Meyer's Loop asymmetries. Epilepsy Res 2014;108:872-82.
25. Basser PJ. Inferring microstructural features and the physiological state of tissues from diffusion-weighted images. NMR Biomed 1995;8:333-44.
26. Mori S, Zhang J. Principles of diffusion tensor imaging and its applications to basic neuroscience research. Neuron 2006;51:527-39.
27. Mori S, van Zij PC. Fiber tracking: principles and strategies - a technical review. NMR Biomed 2002;15:468-80.
28. Conturo TE, Lori NF, Cull TS, Akbudak E, Snyder AZ, Shimony JS, McKinstry RC, Burton H, Raichle ME. Tracking neuronal fiber pathways in the living human brain. Proc Natl Acad Sci U S A 1999;96:10422-7.
29. Jones DK. Studying connections in the living human brain with diffusion MRI. Cortex 2008;44:936-52.
30. Chen X, Weigel D, Ganslandt O, Fahlbusch R, Buchfelder M, Nimsky C. Diffusion tensor-based fiber tracking and intraoperative neuronavigation for the resection of a brainstem cavernous angioma. Surg Neurol 2007;68:285-91; discussion 291.
31. Lee SK, Kim DI, Mori S, Kim J, Kim HD, Heo K, Lee BI. Diffusion tensor MRI visualizes decreased subcortical fiber connectivity in focal cortical dysplasia. Neuroimage 2004;22:1826-9.
32. Lo CY, Chao YP, Chou KH, Guo WY, Su JL, Lin CP. DTI-based virtual reality system for neurosurgery. Conf Proc IEEE Eng Med Biol Soc 2007;2007:1326-9.
33. Melhem ER, Mori S, Mukundan G, Kraut MA, Pomper MG, van Zijl PC. Diffusion tensor MR imaging of the brain and white matter tractography. AJR Am J Roentgenol 2002;178:3-16.
34. Nguyen TH, Yoshida M, Stievenart JL, Iba-Zizen MT, Bellinger L, Abanou A, Kitahara K, Cabanis EA. MR tractography with diffusion tensor imaging in clinical routine. Neuroradiology 2005;47:334-43.

35. Nimsky C, Ganslandt O, Fahlbusch R. Implementation of fiber tract navigation. Neurosurgery 2006;58:ONS-292-303; discussion ONS-303-4.
36. Nimsky C, Ganslandt O, Hastreiter P, Wang R, Benner T, Sorensen AG, Fahlbusch R. Preoperative and intraoperative diffusion tensor imaging-based fiber tracking in glioma surgery. Neurosurgery 2005;56:130-7; discussion 138.
37. Okada T, Mikuni N, Miki Y, Kikuta K, Urayama S, Hanakawa T, Fushimi Y, Yamamoto A, Kanagaki M, Fukuyama H, Hashimoto N, Togashi K. Corticospinal tract localization: integration of diffusion-tensor tractography at 3-T MR imaging with intraoperative white matter stimulation mapping--preliminary results. Radiology 2006;240:849-57.
38. Jones DK, Cercignani M. Twenty-five pitfalls in the analysis of diffusion MRI data. NMR Biomed 2010;23:803-20.
39. De Panfilis C, Schwarzbauer C. Positive or negative blips? The effect of phase encoding scheme on susceptibility-induced signal losses in EPI. Neuroimage 2005;25:112-21.
40. Weiskopf N, Hutton C, Josephs O, Turner R, Deichmann R. Optimized EPI for fMRI studies of the orbitofrontal cortex: compensation of susceptibility-induced gradients in the readout direction. MAGMA 2007;20:39-49.
41. Jones DK. The effect of gradient sampling schemes on measures derived from diffusion tensor MRI: a Monte Carlo study. Magn Reson Med 2004;51:807-15.
42. Landman BA, Farrell JA, Jones CK, Smith SA, Prince JL, Mori S. Effects of diffusion weighting schemes on the reproducibility of DTI-derived fractional anisotropy, mean diffusivity, and principal eigenvector measurements at 1.5T. Neuroimage 2007;36:1123-38.
43. Yamamoto A, Miki Y, Urayama S, Fushimi Y, Okada T, Hanakawa T, Fukuyama H, Togashi K. Diffusion tensor fiber tractography of the optic radiation: analysis with 6-, 12-, 40-, and 81-directional motion-probing gradients, a preliminary study. AJNR Am J Neuroradiol 2007;28:92-6.
44. Catani M, Howard RJ, Pajevic S, Jones DK. Virtual in vivo interactive dissection of white matter fasciculi in the human brain. Neuroimage 2002;17:77-94.
45. Behrens TE, Berg HJ, Jbabdi S, Rushworth MF, Woolrich MW. Probabilistic diffusion tractography with multiple fibre orientations: What can we gain? Neuroimage 2007;34:144-55.
46. Behrens TE, Woolrich MW, Jenkinson M, Johansen-Berg H, Nunes RG, Clare S, Matthews PM, Brady JM, Smith SM. Characterization and propagation of uncertainty in diffusion-weighted MR imaging. Magn Reson Med 2003;50:1077-88.
47. Descoteaux M, Angelino E, Fitzgibbons S, Deriche R.Regularized, fast, and robust analytical Q-ball imaging. Magn Reson Med 2007;58:497-510.
48. Tournier JD, Calamante F, Connelly A. Robust determination of the fibre orientation distribution in diffusion MRI: non-negativity constrained super-resolved spherical deconvolution. Neuroimage 2007;35:1459-72.
49. Wilkins B, Lee N, Gajawelli N, Law M, Leporé N. Fiber estimation and tractography in diffusion MRI: Development of simulated brain images and comparison of multi-fiber analysis methods at clinical b-values. Neuroimage 2015;109:341-56.
50. Tournier JD, Calamante F, Connelly A. MRtrix: diffusion tractography in crossing fiber regions. Int J Imaging Syst Technol 2012;22:53-66.
51. Yamamoto T, Yamada K, Nishimura T, Kinoshita S. Tractography to depict three layers of visual field trajectories to the calcarine gyri. Am J Ophthalmol 2005;140:781-5.
52. Nilsson D, Starck G, Ljungberg M, Ribbelin S, Jönsson L, Malmgren K, Rydenhag B. Intersubject variability in the anterior extent of the optic radiation assessed by tractography. Epilepsy Res 2007;77:11-6.
53. Taoka T, Sakamoto M, Nakagawa H, Nakase H, Iwasaki S, Takayama K, Taoka K, Hoshida T, Sakaki T, Kichikawa K. Diffusion tensor tractography of the Meyer loop in cases of temporal lobe resection for temporal lobe epilepsy: correlation between postsurgical visual field defect and anterior limit of Meyer loop on tractography. AJNR Am J Neuroradiol 2008;29:1329-34.
54. Chen X, Weigel D, Ganslandt O, Buchfelder M, Nimsky C. Prediction of visual field deficits by diffusion tensor imaging in temporal lobe epilepsy surgery. Neuroimage 2009;45:286-97.
55. Sherbondy AJ, Dougherty RF, Napel S, Wandell BA. Identifying the human optic radiation using diffusion imaging and fiber tractography. J Vis 2008;8:12.1-11.
56. Yogarajah M, Focke NK, Bonelli S, Cercignani M, Acheson J, Parker GJ, Alexander DC, McEvoy AW, Symms MR, Koepp MJ, Duncan JS. Defining Meyer's loop-temporal lobe resections, visual field deficits and diffusion tensor tractography. Brain 2009;132:1656-68.
57. Anastasopoulos C, Reisert M, Kiselev VG, Nguyen-Thanh T, Schulze-Bonhage A, Zentner J, Mader I. Local and global fiber tractography in patients with epilepsy. AJNR Am J Neuroradiol 2014;35:291-6.

58. Lilja Y, Ljungberg M, Starck G, Malmgren K, Rydenhag B, Nilsson DT. Visualizing Meyer's loop: A comparison of deterministic and probabilistic tractography. Epilepsy Res 2014;108:481-90.
59. Borius PY, Roux FE, Valton L, Sol JC, Lotterie JA, Berry I. Can DTI fiber tracking of the optic radiations predict visual deficit after surgery? Clin Neurol Neurosurg 2014;122:87-91.
60. Winston GP, Mancini L, Stretton J, Ashmore J, Symms MR, Duncan JS, Yousry TA. Diffusion tensor imaging tractography of the optic radiation for epilepsy surgical planning: a comparison of two methods. Epilepsy Res 2011;97:124-32.
61. Schulz G, Crooijmans HJ, Germann M, Scheffler K, Müller-Gerbl M, Müller B. Three-dimensional strain fields in human brain resulting from formalin fixation. J Neurosci Methods 2011;202:17-27.
62. Dyrby TB, Søgaard LV, Parker GJ, Alexander DC, Lind NM, Baaré WF, Hay-Schmidt A, Eriksen N, Pakkenberg B, Paulson OB, Jelsing J. Validation of in vitro probabilistic tractography. Neuroimage 2007;37:1267-77.
63. Winston GP, Daga P, Stretton J, Modat M, Symms MR, McEvoy AW, Ourselin S, Duncan JS. Optic radiation tractography and vision in anterior temporal lobe resection. Ann Neurol 2012;71:334-41.
64. Powell HW, Parker GJ, Alexander DC, Symms MR, Boulby PA, Wheeler-Kingshott CA, Barker GJ, Koepp MJ, Duncan JS. MR tractography predicts visual field defects following temporal lobe resection. Neurology 2005;65:596-9.
65. Thudium MO, Campos AR, Urbach H, Clusmann H. The basal temporal approach for mesial temporal surgery: sparing the Meyer loop with navigated diffusion tensor tractography. Neurosurgery 2010;67:385-90.
66. Siu DY, Zhu XL, Abrigo J, Wang YX, Leung JCS, Mak CHK, Poon WS. The use of diffusion tensor tractography to prevent visual field defect in epilepsy surgery - a prospective study. J Med Imaging Radiat Oncol 2012;56:22-47.
67. Winston GP, Daga P, White MJ, Micallef C, Miserocchi A, Mancini L, Modat M, Stretton J, Sidhu MK, Symms MR, Lythgoe DJ, Thornton J, Yousry TA, Ourselin S, Duncan JS, McEvoy AW. Preventing visual field deficits from neurosurgery. Neurology 2014;83:604-11.

Cite this article as: Lilja Y, Nilsson DT. Strengths and limitations of tractography methods to identify the optic radiation for epilepsy surgery. Quant Imaging Med Surg 2015;5(2):288-299. doi: 10.3978/j.issn.2223-4292.2015.01.08

